AIP | The Journal of Chemical Physics

Electronimpact ionization cross sections of the SiF3 free radical

Todd R. Hayes, Randy J. Shul, Frank A. Baiocchi, Robert C. Wetzel, and Robert S. Freund

Citation: The Journal of Chemical Physics **89**, 4035 (1988); doi: 10.1063/1.454836
View online: http://dx.doi.org/10.1063/1.454836
View Table of Contents: http://scitation.aip.org/content/aip/journal/jcp/89/7?ver=pdfcov
Published by the AIP Publishing

Electron-impact ionization cross sections of the SiF_3 free radical

Todd R. Hayes, Randy J. Shul, Frank A. Baiocchi, Robert C. Wetzel, and Robert S. Freund
AT&T Bell Laboratories, Murray Hill, New Jersey 07974

(Received 12 May 1988; accepted 15 June 1988)

Absolute cross sections for electron-impact ionization of the SiF_3 free radical from threshold to 200 eV are presented for formation of the parent SiF_3^+ ion and the fragment SiF_2^+, SiF^+, and Si^+ ions. A 3 keV beam of SiF_3 is prepared by near-resonant charge transfer of SiF_3^+ with 1,3,5-trimethylbenzene. The beam contains only ground electronic state neutral radicals, but with as much as 1.5 eV of vibrational energy. The absolute cross section for formation of the parent ion at 70 eV is 0.67 ± 0.09 Å^2. At 70 eV the formation of SiF_2^+ is the major process, having a cross section 2.51 ± 0.02 times larger than that of the parent ion, while the SiF^+ fragment has a cross section 1.47 ± 0.08 times larger than the parent. Threshold measurements show that ion pair dissociation processes make a significant contribution to the formation of positively charged fragment ions.

I. INTRODUCTION

The SiF_3 free radical is one of the reactive species which is expected to be important in the gas phase chemistry of the silicon–fluorine system. This chemistry occurs, for example, in plasma processing of silicon integrated circuits with fluorine containing gases,[1] and in ion-assisted etching of silicon surfaces.[2] Among the unmeasured fundamental data on SiF_3 are the absolute electron impact ionization cross sections for parent and fragment ions, which are needed for modeling, and the relative fragment-to-parent ion ratios, which are needed for mass spectrometry of the neutral species.

Little information exists on electron impact ionization of free radicals due to the difficulties in forming and handling these highly reactive species. Measurements of dissociative ionization are further complicated by the difficulty of quantitatively collecting the fragments. The fast neutral beam technique used here alleviates these problems; it has been used previously in our laboratory to measure ionization cross sections of the SiF, CD_2, and CD_3 radicals.[3,4] The method has been well tested by numerous measurements on the rare gases.[5] In this paper we report absolute electron impact ionization cross section measurements for the processes $SiF_3 + e^- \rightarrow SiF_3^+$, SiF_2^+, SiF^+, and Si^+ from threshold to 200 eV.

II. EXPERIMENTAL

A. Apparatus

The apparatus used in the present study has been described previously[4,5]; therefore, only the details relevant to the study of the SiF_3 free radical and some recent apparatus improvements are discussed. Briefly, ions are extracted from a high pressure dc discharge (Colutron[6]) and accelerated to 3 keV. The ionic species of interest are velocity filtered by a Wien filter and passed through a region of high pressure ($\sim$0.1 mTorr) where charge transfer neutralization occurs. The neutral beam, with a flux of about 10^{10} s^{-1}, passes through a beam-defining aperture and is crossed and ionized by a well-characterized electron beam. After the ions are focused at the entrance of a hemispherical energy analyzer by an einzel lens, they are separated by their energy (mass to charge ratio), and detected with a channeltron electron multiplier (CEM) operating in the pulse counting mode.

The vacuum has been improved significantly by replacing the diffusion pump in the experimental main chamber with a cryopump, by continuing use of a liquid nitrogen cold finger, and by periodic, mild bakeouts (100 °C). The result has been an overall decrease in the base pressure from $\sim 5 \times 10^{-8}$ to 1×10^{-9} Torr with a working pressure of $\sim 3 \times 10^{-9}$ Torr. Residual gas analysis has shown that H_2O is the principal background species, with lower levels of N_2, CO, O_2, CO_2, and H_2. The decrease of background gas in the main chamber has resulted in much improved signal-to-noise ratios.

An additional change was relocation of the charge transfer cell from the middle vacuum chamber to the source chamber. This was done to reduce the amount of neutral dissociation products from the ion beam which contaminate the otherwise pure SiF_3 neutral beam, and to further lower the pressure in the main chamber. Increasing the distance from the charge transfer cell to the electron beam decreases the solid angle subtended by the electron gun entrance aperture and discriminates against collision products scattered by more than $\sim$0.18°. Threshold measurements described below confirm that SiF and SiF_2 are now minor or negligible components of the SiF_3 beam. In our preliminary reports of SiF_3 cross sections[7,8] with the charge transfer cell in the middle chamber, there were significant beam contaminants.

B. Charge transfer neutralization

A number of gases were tried for charge transfer neutralization of SiF_3^+. Based on the criterion of energy resonance and the 9.0–9.4 eV approximate adiabatic ionization potential of SiF_3 (Table I), we tested a number of charge transfer gases with ionization potentials from 8.42–12.0 eV. The gas yielding the largest charge transfer cross section was 1,3,5-trimethylbenzene (abbreviated here as TMB), which has an ionization potential of 8.42 eV and a first photoelectron band extending up to 9.3 eV[9] (Fig. 1). TMB was used

TABLE I. Thermochemical data.

			Footnote
Heats of formation at 298 K (eV)	SiF_4	-16.74 ± 0.01	a
	SiF_3	-10.36 ± 0.22	b
	SiF_2	-6.09 ± 0.13	a
	SiF	-0.21 ± 0.13	a
	Si	4.66 ± 0.08	a
	F	0.82 ± 0.00	a
	F_2	0.00	c
	CH_3SiF_3	$[-12.78]$	d
	CH_3	1.51 ± 0.01	a
Experimental ionization thresholds (eV)	$SiF_3CH_3 \rightarrow SiF_3^+ + CH_3$	13.33 ± 0.05	e
	$SiF_4 \rightarrow SiF_3^+ + F$	16.20 ± 0.1	f
	$SiF_2 \rightarrow SiF_2^+$	10.78 ± 0.05	g
	$SiF \rightarrow SiF^+$	7.28 ± 0.05	h
	$Si \rightarrow Si^+$	8.15 ± 0.00	i
	$F^- \rightarrow F$	3.399 ± 0.002	j
	$F_2^- \rightarrow F_2$	3.08 ± 0.10	k
Derived thresholds (eV)	$SiF_3 \rightarrow SiF_3^+$	9.4 ± 0.22	l
		9.0 ± 0.24	m
	$SiF_3 \rightarrow SiF_2^+ + F^-$	12.47 ± 0.26	
	$SiF_3 \rightarrow SiF_2^+ + F$	15.87 ± 0.26	
	$SiF_3 \rightarrow SiF^+ + F_2^-$	14.35 ± 0.28	
	$SiF_3 \rightarrow SiF^+ + F + F^-$	15.66 ± 0.28	
	$SiF_3 \rightarrow SiF^+ + F_2$	17.43 ± 0.26	
	$SiF_3 \rightarrow SiF^+ + F + F$	19.06 ± 0.28	
	$SiF_3 \rightarrow Si^+ + F_2 + F^-$	20.59 ± 0.23	
	$SiF_3 \rightarrow Si^+ + F_2^- + F$	20.91 ± 0.25	
	$SiF_3 \rightarrow Si^+ + F_2 + F$	23.99 ± 0.23	
	$SiF_3 \rightarrow Si^+ + F + F + F$	25.62 ± 0.25	

[a] Reference 23.

[b] Reference 24.

[c] Definition.

[d] Reference 23. JANAF does not list an uncertainty for this value.

[e] Reference 21.

[f] Reference 20.

[g] N. P. C. Westwood, Chem. Phys. Lett. **25**, 558 (1974).

[h] K. P. Huber and G. H. Herzberg, *Molecular Spectra and Molecular Structure* (Van Nostrand Reinhold, New York, 1979).

[i] C. M. Brown, S. G. Tilford, R. Tousey, and M. L. Ginter, J. Opt. Soc. Am. **64**, 1665 (1974).

[j] H. Hotop and W. C. Lineberger, J. Phys. Chem. Ref. Data **14**, 731 (1985).

[k] W. A. Chupka and J. Berkowitz, J. Chem. Phys. **55**, 2724 (1971).

[l] Based on dissociative ionization of CH_3SiF_3. The uncertainty is an estimate due to the absence of an uncertainty for the ΔH_f of CH_3SiF_3.

[m] Based on dissociative ionization of SiF_4.

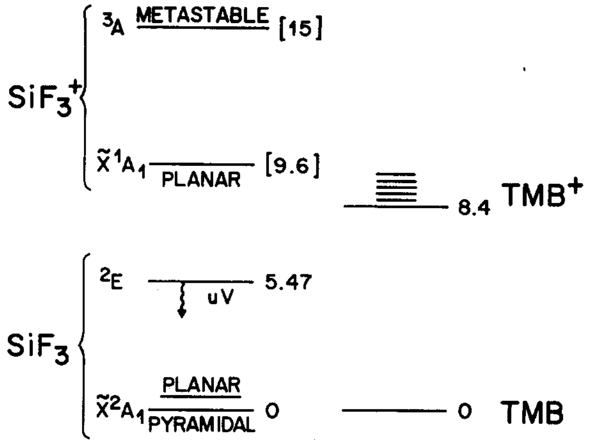

FIG. 1. Schematic potential energy diagram showing the near-resonant charge transfer of SiF_3^+ with TMB (1,3,5-trimethylbenzene).

for all measurements reported here. Propane, cyclopropane, and ethylene displayed charge transfer cross sections with SiF_3^+ which were comparable to each other but approximately ten times smaller than that with TMB.

Since charge transfer neutralization of ground state SiF_3^+ by TMB is near resonant, it is expected to yield neutral SiF_3 predominantly in the ground electronic state. The lowest known excited electronic state of neutral SiF_3 is 5.47 eV above the ground state with a radiative lifetime much shorter than the time-of-flight to the electron beam.[10,11] The lowest quartet state has never been observed, but it too should lie near 5 eV above the ground state, based on its possible orbital configuration. Both of these states lie only about 4 eV below the ground state ion, and so should not resonantly charge transfer with TMB. They could form, however, if the ion source produces large quantities of electronically excited SiF_3^+. Although we are unable to find any direct experimental or theoretical data on the excited states of SiF_3^+, analogy with BF_3[12,13] suggests that the first excited state of SiF_3^+ is ~6 eV above its ground state, i.e., 15 eV above the ground state neutral. This state would probably be a long-lived triplet and its resonant neutralization by TMB could form states of SiF_3 5–6 eV above the ground state. Such excited states of SiF_3 should be revealed by a lowered ionization threshold, and its absence (see below) suggests that there is no substantial amount of electronically excited SiF_3 in the neutral beam and no substantial amount of excited SiF_3^+ in the ion beam.

Vibrational excitation of the SiF_3 beam is probable, however, because the geometries of SiF_3^+ and SiF_3 differ considerably (Fig. 2). SiF_3^+ presumably forms in the ion source with considerable energy in its inversion mode, since it forms from tetrahedral SiF_4 and its equilibrium geometry is planar.[14] The ground state equilibrium geometry of neutral SiF_3 is out-of-plane with an inversion barrier which by analogy with CF_3[15–17] and $SiCl_3$[18] should be between about 0.5 and 2.0 eV. Charge transfer from the vibrationally excited ion can (assuming it is a vertical transition) therefore produce the ground state neutral near its pyramidal equilibrium geometry while charge transfer from an equilibrated (planar) ion can produce the ground state neutral near the peak of its inversion barrier. A significant distribution of vibrational energy is thus expected even though some collisional relaxation may occur in the ion source.

C. Fragment collection efficiency

Accurate absolute cross section measurements require quantitative collection of all ions produced by electron im-

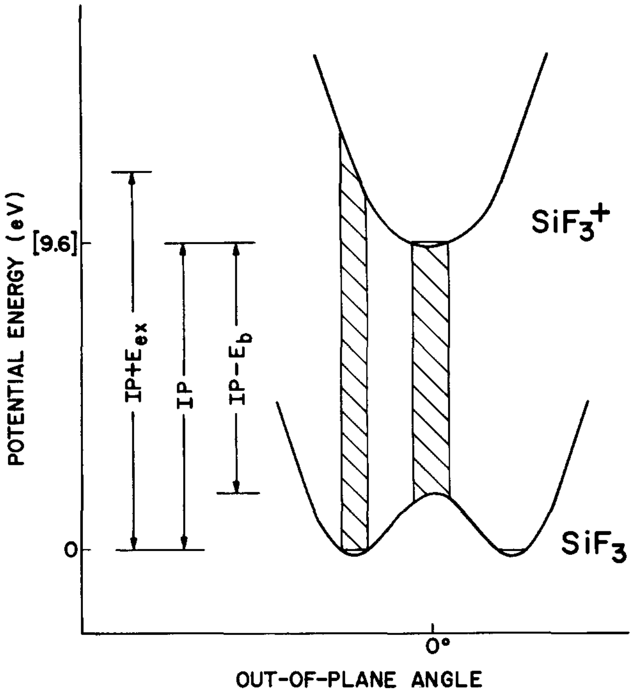

FIG. 2. Schematic diagram of SiF_3 (pyramidal ground state) and SiF_3^+ (planar ground state) and the relationship of the vertical ionization energy ($IP + E_{ex}$ or $IP - E_b$) to the adiabatic ionization potential (IP), vibrational excitation (E_{ex}), and barrier height (E_b).

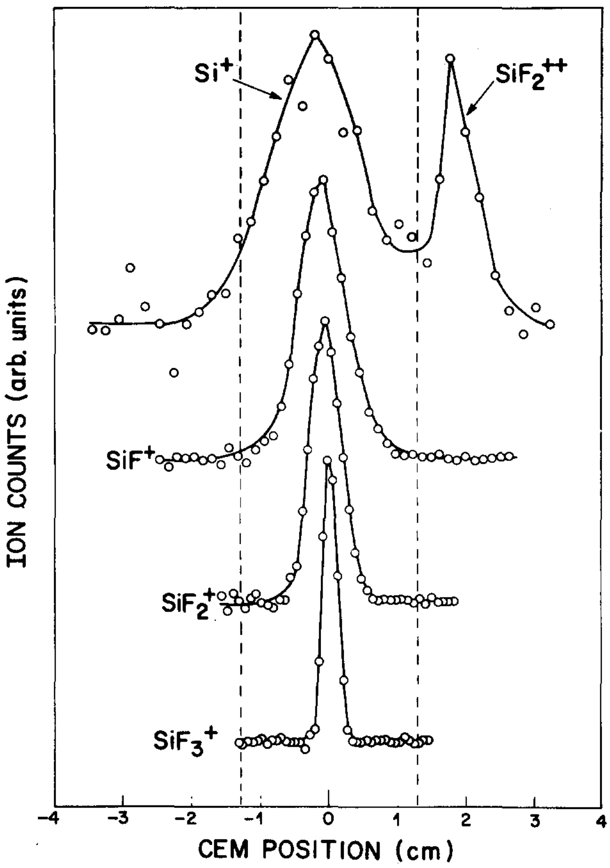

FIG. 3. Mass spectra of ions produced by ionization of SiF_3 by 100 eV electrons, over the ranges (from top to bottom) 20–36, 40–56, 60–75, and 80–96 amu. These mass spectra are obtained by scanning the hemispherical energy analyzer over narrow ranges with a slit positioned in front of the CEM (channel electron multiplier). The equivalent width of the full 2.5 cm diameter CEM entrance cone is indicated by dashed lines, demonstrating that in the absence of the slit, SiF_3^+, SiF_2^+, and SiF^+ are completely collected, Si^+ is nearly completely collected, and SiF_2^{++} is resolved from Si^+.

pact. Scans of each mass-separated ion across a slit in front of the CEM are used to measure their profiles and either confirm complete collection or determine the fraction collected. The parent ion beam, SiF_3^+, remains well collimated, but kinetic energy released by the dissociation process introduces an angular divergence and energy spread into the fragment ion beams, increasing as their masses decrease. Figure 3 shows the measured profiles; 100% of the SiF_3^+, SiF_2^+, and SiF^+ beams are collected by the 2.5 cm CEM entrance cone, but only $\sim 75 \pm 10\%$ of the Si^+ fragment is collected.

The counting efficiency ϵ of the CEM is also of concern. We conclude for several reasons that the detection efficiency is independent of the fragment species. Although it is not measured directly, it is estimated to be near unity, based on the observed saturation of count rate as the CEM voltage is increased to 3.4 keV. In addition, measured cross sections for all five rare gases[5] agree with previous literature measurements, even though their masses and therefore their velocities are considerably different. And finally, there are several literature reports[19] of near unity CEM efficiencies for ion energies above 4.5 keV, as is the case here ($3m/M$ keV beam energy + 3.4 keV acceleration to the CEM, where m is the mass of the fragment and M is the mass of the parent). To allay an additional concern, invariance of the CEM efficiency with position is demonstrated by scanning tightly focused ion beams across the face of the CEM with the hemispherical energy analyzer. Such probes have shown that the efficiency over the entire 2.5 cm surface is constant to within about $\pm 1.5\%$.

D. Calibration of the neutral flux measurement

The method of measuring the neutral beam flux has been modified slightly to simplify the procedure and reduce the effect of beam intensity fluctuations. The pyroelectric sensitivity is now calibrated by measuring its response to neutral rare gas beams whose flux is calculated from their known ionization cross sections.[5] Therefore, the calibration of the pyroelectric sensitivity does not require exposure to intense ion beams which generate drifts and instabilities due to surface charging and deposition of insulating films. Twenty-one calibration measurements with Ar, Kr, Xe, and SiF, made over a period of one week, yielded a sensitivity constant ϕ of 3.37 ± 0.14 V/W.

E. Cross section measurements

The technique for the measurement of absolute cross sections in our laboratory has been discussed in detail previously.[4,5] The cross section σ in Å^2 for the SiF_3^+ parent ion is given by:

$$\sigma = \frac{C_{corr}\phi E^{3/2} D\, 3.51\times 10^{-4}}{I_e F V^0_{ch} M^{1/2}}, \quad (1)$$

where C_{corr} is the corrected ion counts per second, ϕ is the pyroelectric sensitivity in V/W, E is the beam energy in eV, D is the duty cycle of the chopper, I_e is the electron current in μA, F is the geometric overlap of the electron and neutral beams with units of cm^{-1}, V^0_{ch} is the response of the pyroelectric in μV to the chopped neutral beam, and M is the mass of the ion in atomic units. The constant contains several factors in addition to fundamental constants, namely the CEM detection efficiency, the electron reflection coefficient from the electron gun anode, and the neutral transmission probability through the hemispherical energy analyzer to the pyroelectric detector.

III. RESULTS

Absolute cross sections were measured for the formation of SiF_3^+, SiF_2^+, SiF^+, and Si^+ from SiF_3 by electron impact ionization. The procedure was to initially measure the thresholds, in order to determine the amount of internal energy in the beam, verify the processes involved, and check the purity of the beam. Relative cross sections from 0 to 200 eV were measured next, for parent and fragment ions. Finally, the absolute cross sections for parent ionization and the ratios of fragment-to-parent cross sections were measured at selected electron energies and used to normalize the relative 0 to 200 eV cross sections.

A. Thresholds

Measured thresholds are shown in Fig. 4. The data are each the sum of five independent runs taken over a period of several weeks, each representing a total of about 10 h of signal accumulation. The energy scale of each independent run was calibrated by a rare gas threshold measurement immediately before or after it. These calibrated energy scales agreed with those calculated by Eq. (1) of Ref. 4 to within 0.2 eV. The Si^+ signal-to-noise was too low to permit the measurement of a meaningful threshold.

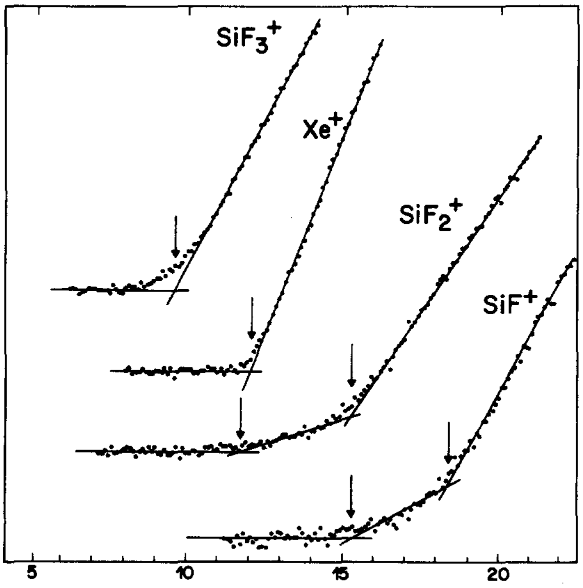

FIG. 4. Thresholds for ionization of SiF_3 to its parent and fragment ions, together with the xenon threshold used to calibrate the energy scale and determine the electron energy spread.

The SiF_3^+ threshold demonstrates the absence of excited SiF_3 electronic states in the SiF_3 beam, as discussed in Sec. II B. The large amount of curvature, however, does demonstrate a significant amount of vibrational energy. The SiF_3^+ threshold shows curvature over 2 eV while xenon shows it over less than 1 eV. We base our interpretation of this threshold on Fig. 2, which shows the potential energy curves for the ion and neutral ground states in the inversion mode. The adiabatic ionization potential (IP) is inaccessible by a vertical transition. Vertical ionization of the equilibrated (pyramidal) neutral takes place to a pyramidal ion, with a range of vibrational excitation energy around the value $IP + E_{ex}$. Ionization of an inverting neutral would take place preferentially from a near-planar geometry, with a range of energies around $IP - E_b$, where E_b is the height of the inversion barrier. The threshold curvature, therefore, spans a rather poorly defined range $E_{ex} + E_b$, centered approximately at IP. Using this model as a guide, we take 9.6 ± 0.6 eV as the value of IP, the intercept of the two straight lines shown in Fig. 4. There is no direct measurement of the SiF_3 ionization potential in the literature, so for comparison purposes, a value must be calculated from thermochemical data. Combining the 16.20 ± 0.1 eV dissociative ionization threshold[20] of $SiF_4 \rightarrow SiF_3^+ + F$ with the appropriate heats of formation from Table I, we calculate 9.0 ± 0.24 eV. Combining the 13.33 ± 0.05 eV dissociative ionization threshold[21] of $CH_3SiF_3 \rightarrow SiF_3^+ + CH_3$ with the appropriate heats of formation gives 9.4 ± 0.23 eV. The ionization potential derived by Weber and Armentrout[22] is 9.99 ± 0.24 eV. Our present measurement agrees with all three.

The threshold for formation of SiF_2^+ from electron impact ionization of SiF_3 is shown in Fig. 4. There appear to be two distinct processes, each occurring with slight curvature due to vibrational excitation of the parent neutral beam. The major threshold for production of SiF_2^+ is at 15.2 ± 0.5 eV. Based on the thermochemical data in Table I, this threshold is assigned as $SiF_3 \rightarrow SiF_2^+ + F$ which has a calculated energy of 15.87 ± 0.26 eV, the difference being ascribable to poor signal-to-noise and the uncertainty introduced by vibrational excitation. The lower threshold at 11.7 ± 0.5 eV represents approximately 21% of the SiF_2^+ production, and lies 3.5 eV below the major threshold. The 3.4 eV electron affinity of fluorine strongly supports the assignment as ion pair production, $SiF_3 \rightarrow SiF_2^+ + F^-$. From Table I, the calculated energy of this process is 12.47 ± 0.26 eV. A very small signal between 10.5 and 11.7 eV, of questionable significance, could be explained as ionization of an SiF_2 impurity in the SiF_3 beam, with an ionization potential of 10.78 ± 0.05 eV. Clearly, there is very little SiF_2 in the beam.

The threshold for the formation of SiF^+ from the electron impact ionization of SiF_3 is shown in Fig. 4. At least two processes are observed with significant curvature at threshold for each. The major threshold for the production of SiF^+

TABLE II. Measured values of the fragment to parent ion ratios, and of the absolute cross section for $SiF_3 \rightarrow SiF_3^+$.

Electron energy (eV)		SiF_2^+/SiF_3^+ ($\pm 1\%$)	SiF^+/SiF_3^+ ($\pm 7\%$)	Si^+/SiF_3^+ ($\pm 18\%$)	Absolute cross section (Å^2)
50	measured value	2.04	1.27	0.18	0.73 ± 0.11
	# measurements	(3)	(3)	(2)	(1)
70	measured value	2.51	1.47	0.27	0.67 ± 0.09
	# measurements	(3)	(3)	(2)	(11)
100	measured value	2.93	1.74	0.36	0.67 ± 0.10
	# measurements	(3)	(3)	(2)	(1)

is at 18.3 ± 0.5 eV. This is in the range of both $SiF_3 \rightarrow SiF^+ + F_2$ at a calculated energy of 17.43 ± 0.26 eV, and $SiF_3 \rightarrow SiF^+ + F + F$ at 19.06 ± 0.28 eV. The lower threshold at 15.3 ± 0.6 eV represents approximately 30% of the SiF^+ production. The assignment appears to be one or both of the ion pair processes $SiF_3 \rightarrow SiF^+ + F_2^-$ and $SiF^+ + F + F^-$ at 14.35 ± 0.28 and 15.66 ± 0.28 eV, respectively. In each case we favor the lower energy process because it involves dissociation into only two fragments rather than three, and because the difference between the lower process and the observed threshold can be accounted for by kinetic energy of the fragments.

B. Cross sections

Relative cross sections for the parent and each fragment were measured by sweeping repetitively the electron energy from 0 to 200 eV with 1 eV steps at 0.5 s intervals per step and recording the ion counts. The raw counts were corrected for variation of the electron current, which increases from about 100 μA at 10 eV to about 400 μA at 200 eV, and for small variations in the neutral beam flux which remains approximately constant. Several runs each lasting from 1 to 3 h were added together to improve the signal-to-noise. Small corrections to the shapes were made in accordance with Eq. (15) of Ref. 5; these corrections are under 5% below 50 eV and above 150 eV, and are negligible between 50 and 150 eV.

Table II lists the measured ratios of fragment-to-parent ions at 50, 70, and 100 eV electron energy. The measurement of ion ratios is probably one of the most accurate measurements in this study since many quantities in Eq. (1) cancel out (the neutral beam flux, the electron beam current, and the overlap). The uncertainty of a ratio measurement must include the collection efficiency of the fragment ion in addition to the statistical uncertainty. The percent uncertainties are $\pm 1\%$, $\pm 7\%$, and $\pm 18\%$ for the ratios of SiF_2^+/SiF_3^+, SiF^+/SiF_3^+, and Si^+/SiF_3^+, respectively.

The absolute cross section for parent ionization, $SiF_3 \rightarrow SiF_3^+$ is also given in Table II. Eleven measurements were made at an electron energy of 70 eV, yielding an average value of 0.67 Å^2 with a one-standard-deviation statistical uncertainty of $\pm 7.5\%$. Combined with our estimated $\pm 12\%$ systematic uncertainty, this gives an overall uncertainty of $\pm 14.2\%$ and a cross section of 0.67 ± 0.09 Å^2.

The cross section results are presented in Fig. 5 and in Table III. The parent ion shape was normalized to the 70 eV absolute cross section, and then the fragment ion shapes were normalized using the 70 eV fragment-to-parent ion ratios. The total uncertainties of the cross section vs energy curves are determined from the $\pm 14.2\%$ uncertainty of the absolute cross section, the $\pm 1\%$, 7%, and 18% uncertainties of the ratios, and the estimated $\pm 5\%$ uncertainties in the relative cross section shapes. The total uncertainties at electron energy more than 10 eV above threshold are $\pm 15\%$, $\pm 15\%$, $\pm 16\%$, and $\pm 23\%$ for the formation of SiF_3^+, SiF_2^+, SiF^+, and Si^+, respectively. At electron energies less than 10 eV above threshold, these uncertainties are somewhat larger due to the increased statistical uncertainty. Shapes are verified by SiF_3^+ absolute cross sections measured at 50 and 100 eV, as given in Table II and indicated by triangles in Fig. 5, and also by the ratios measured at 50 and

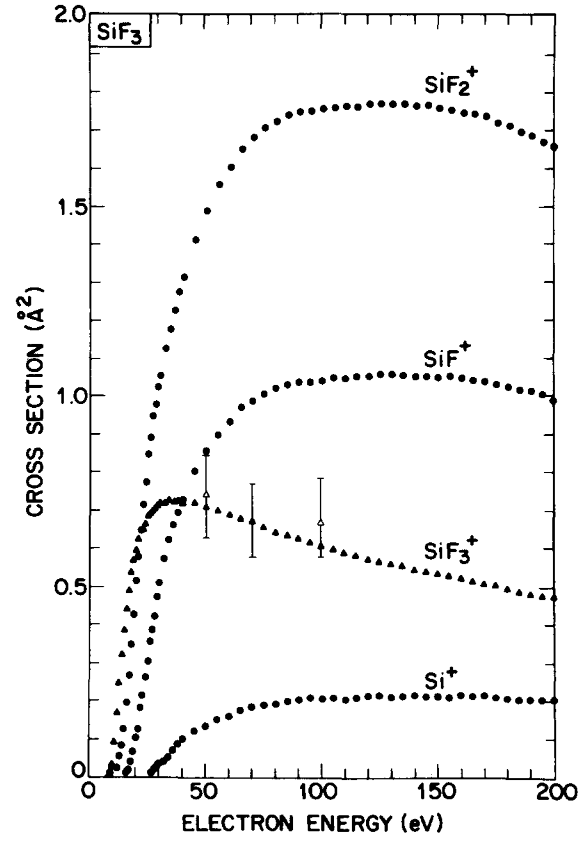

FIG. 5. Electron impact ionization cross sections vs electron energy from threshold to 200 eV for ionization of SiF_3 to its parent and fragment ions.

100 eV (Table II). Within experimental error, these values agree with those calculated from Table III.

No signal was observed for the F^+ fragment ion, implying that the peak cross section for its formation is less than about 0.01 Å². The doubly charged ion SiF_2^{++} gave a weak signal (see Fig. 3). Athough no accurate measurements could be made, we estimate its cross section at 100 eV to be 0.1 Å², within a factor of about 2. This value is probably a lower limit, since doubly charged molecular ions are often observed to predissociate with lifetimes on the order of microseconds, comparable to the time-of-flight to our detector.

TABLE III. Cross sections for electron impact ionization of SiF_3.

Electron energy (eV)	Product ion cross section (Å²)[a]			
	SiF_3^+	SiF_2^+	SiF^+	Si^+
8		0.01		
9	0.01	0.01		
10	0.04	0.01		
11	0.09	0.02		
12	0.17	0.02		
13	0.25	0.06		
14	0.32	0.08	0.01	
15	0.39	0.13	0.01	
16	0.44	0.19	0.01	
17	0.49	0.27	0.02	
18	0.54	0.35	0.04	
19	0.57	0.43	0.07	
20	0.60	0.51	0.10	
21	0.63	0.58	0.13	
22	0.65	0.65	0.18	
23	0.65	0.71	0.21	
24	0.66	0.77	0.26	
25	0.69	0.84	0.30	
26	0.69	0.89	0.35	
27	0.70	0.95	0.39	0.01
28	0.70	0.98	0.42	0.02
29	0.71	1.02	0.47	0.03
30	0.72	1.06	0.51	0.04
32	0.72	1.13	0.57	0.04
34	0.72	1.18	0.62	0.05
36	0.72	1.23	0.66	0.07
38	0.72	1.28	0.69	0.09
40	0.72	1.32	0.73	0.10
45	0.72	1.41	0.80	0.12
50	0.71	1.49	0.86	0.13
55	0.70	1.56	0.90	0.15
60	0.69	1.61	0.93	0.16
65	0.68	1.65	0.97	0.17
70	0.67	1.68	0.99	0.18
75	0.66	1.71	1.01	0.19
80	0.64	1.73	1.02	0.19
85	0.63	1.74	1.03	0.20
90	0.63	1.75	1.04	0.20
95	0.61	1.75	1.04	0.21
100	0.60	1.76	1.04	0.20
105	0.60	1.76	1.05	0.21
110	0.59	1.77	1.05	0.20
115	0.58	1.76	1.06	0.21
120	0.57	1.77	1.06	0.21
125	0.57	1.77	1.06	0.21
130	0.56	1.77	1.06	0.21
135	0.55	1.77	1.06	0.21
140	0.55	1.77	1.06	0.21
145	0.54	1.77	1.06	0.21
150	0.54	1.76	1.05	0.21
155	0.53	1.75	1.06	0.21
160	0.52	1.75	1.05	0.21
165	0.52	1.75	1.04	0.21
170	0.51	1.74	1.04	0.21
175	0.50	1.72	1.04	0.21
180	0.50	1.71	1.03	0.21
185	0.49	1.70	1.02	0.21
190	0.48	1.69	1.02	0.21
195	0.48	1.67	1.01	0.20
200	0.48	1.66	0.99	0.20

[a] The total uncertainties of these cross sections are discussed within the text.

IV. DISCUSSION

The only previous measurements of SiF_3 ionization cross sections are two preliminary reports of this work. The results from Ref. 7 (Table IV) differ somewhat from the present values, but are close to or within the one-standard-deviation error limits. A major contributor to the errors in Ref. 8 was the presence of SiF and SiF_2 contaminants in the SiF_3 beam. These contaminants lowered the measured absolute cross section value because they added to the measured neutral beam flux, but did not add to the SiF_3^+ ion count. Similarly, they increased the values of the SiF_2^+/SiF_3^+ and SiF^+/SiF_3^+ ratios. Another possible source of the difference is that previously propane was used as the charge transfer gas. Recent measurements using propane suggest the same absolute cross section and slightly larger ratios than the measurements with TMB as a charge transfer gas, but they have substantially greater noise and scatter. Since the ratio differences are comparable to the scatter of the propane measurements, we conclude that the present values using TMB are to be preferred.

The effect of SiF_3 vibrational energy on the measured cross sections is unknown. It is certainly possible that ionization of excited vibrational levels gives different dissociative ionization patterns than ionization of the ground state. Attempts were made to vary the amount of vibrational excitation by using several different charge transfer gases, but within the limitations of signal-to-noise, no reproducible changes in the absolute cross section or ratios were observed. This is not a definitive test, since threshold measurements were not sufficiently sensitive to determine whether or not the degree of vibrational excitation did change. One can argue that the effects of vibrational excitation may be unimportant for the application of these results to SiF_3 in plasma or sputtering systems, since in these energetic and poorly defined environments, the formation mechanisms of SiF_3 might produce a vibrational distribution similar to that obtained here.

One final observation has to do with the heat of formation of SiF_3, which has been controversial in the literature. The JANAF tables[23] give $\Delta H_f^{298} = -11.25 \pm 0.17$ eV. Walsh[24] has determined the value to be -10.36 ± 0.22 eV,

TABLE IV. Comparison of present results to preliminary reports.

	Ratios of cross sections (70 eV)		Absolute cross section (Å²)
	SiF_2^+/SiF_3^+	SiF^+/SiF_3^+	
Reference 7	2.04 ± 0.30	1.39 ± 0.11	0.49 ± 0.15
Reference 8	2.73	2.08	0.42
This work	2.51 ± 0.02	1.47 ± 0.08	0.67 ± 0.09

and Schlegel[25] calculates a theoretical value of -10.28 ± 0.04 eV, in excellent agreement with Walsh. Most recently, Weber and Armentrout[22] determined a value of 11.19 ± 0.13 eV, close to the JANAF value. We have used Walsh's value of ΔH_f^{298} to derive Table I. If, instead, we had used the JANAF[23] value, the calculated thresholds for SiF_2^+ would be 13.36 and 16.76 eV, well above our measured values of 11.7 and 15.2 eV. The SiF_3^+ threshold provides no new evidence for the value of ΔH_f, since with the JANAF[23] ΔH_f, the calculated ionization potential would be 9.89 or 10.29 eV (based on dissociative ionization of SiF_4 or CH_3SiF_3, respectively[20,21]) in agreement with the measured 9.6 ± 0.6 eV.

V. CONCLUSIONS

The absolute cross sections and fragmentation pattern are reported for the first time for the electron impact ionization of the SiF_3 free radical from threshold to 200 eV. The degree of vibrational excitation of the parent radical has not been quantitatively determined, however curvature in the parent ion threshold region suggests it is approximately 1.5 eV. Although the effect of vibrational excitation on the cross sections for ionization and dissociative ionization of SiF_3 is not known, we have no experimental evidence to suggest that it is large. With this stipulation, we assign the accuracies of the electron impact ionization cross sections from $\pm 15\%$ for the parent to $\pm 23\%$ for the Si fragment.

[1] H. F. Winters and F. A. Houle, J. Appl. Phys. **54**, 1218 (1983).
[2] D. J. Oostra, A. Haring, A. E. de Vries, F. H. M. Sanders, and K. Miyake, Appl. Phys. Lett. **46**, 1166 (1985).
[3] F. A. Baiocchi, R. C. Wetzel, and R. S. Freund, Phys. Rev. Lett. **53**, 771 (1984).
[4] T. R. Hayes, R. C. Wetzel, F. A. Baiocchi, and R. S. Freund, J. Chem. Phys. **88**, 823 (1988).
[5] R. C. Wetzel, F. A. Baiocchi, T. R. Hayes, and R. S. Freund, Phys. Rev. A **35**, 559 (1986).
[6] L. Whalin, Nucl. Instrum. Methods **27**, 55 (1964).
[7] R. C. Wetzel, F. A. Baiocchi, R. S. Freund, Bull. Am. Phys. Soc. **30**, 147 (1985).
[8] R. S. Freund, in *Swarm Studies and Inelastic Electron–Molecule Collisions*, edited by L. C. Pitchford, B. V. McKoy, A. Chutjian, and S. Trajmar (Springer, New York, 1987).
[9] T. Koenig and M. Tuttle, J. Org. Chem. **39**, 1308 (1974).
[10] J. L. F. Wang, C. N. Krishnan, and J. L. Margrave, J. Mol. Spectrosc. **48**, 346 (1973).
[11] S. P. So, J. Mol. Struct. **39**, 133 (1977).
[12] D. Goutier and L. A. Burnelle, Chem. Phys. Lett. **18**, 460 (1973).
[13] J. A. Tossell, J. H. Moore, and J. K. Olthoff, Int. J. Quantum Chem. **29**, 346 (1973).
[14] A. D. Walsh, J. Chem. Soc. **1953**, 2301.
[15] D. A. Dixon, J. Chem. Phys. **83**, 6055 (1985).
[16] J. Moc, Z. Latajka, and H. Ratajczak, J. Mol. Struct. **138**, 3353 (1986).
[17] G. L. Gutsev and T. S. Zyubina, Chem. Phys. **83**, 89 (1984).
[18] J. Moc, Z. Latajka, and H. Ratajczak, Chem. Phys. Lett. **136**, 122 (1987).
[19] Discussed in Ref. 5.
[20] J. D. McDonald, C. H. Williams, J. C. Thompson, and J. L. Margrave, Adv. Chem. Ser. **72**, 261 (1968).
[21] M. K. Murphy and J. L. Beauchamp, J. Am. Chem. Soc. **99**, 2085 (1977).
[22] M. E. Weber and P. B. Armentrout, J. Chem. Phys. **88**, 6898 (1988).
[23] JANAF Thermochemical Tables, Third Edition, J. Phys. Chem. Ref. Data **14**, Supplement No. 1 (1985).
[24] R. Walsh, J. Chem. Soc. Faraday Trans. 1 **79**, 2233 (1983).
[25] H. B. Schlegel, J. Phys. Chem. **88**, 6254 (1984).